



Published in final edited form as:

Cell Rep. 2021 August 24; 36(8): 109615. doi:10.1016/j.celrep.2021.109615.

Lateral hypothalamic LEPR neurons drive appetitive but not consummatory behaviors

Justin N. Siemian¹, Miguel A. Arenivar¹, Sarah Sarsfield¹, Cara B. Borja¹, Charity N. Russell¹, Yeka Aponte^{1,2,3,*}

¹Neuronal Circuits and Behavior Unit, National Institute on Drug Abuse Intramural Research Program, National Institutes of Health, Baltimore, MD 21224-6823, USA

²The Solomon H. Snyder Department of Neuroscience, Johns Hopkins University School of Medicine, Baltimore, MD 21205, USA

³Lead contact

SUMMARY

Assigning behavioral roles to genetically defined neurons within the lateral hypothalamus (LH) is an ongoing challenge. We demonstrate that a subpopulation of LH GABAergic neurons expressing leptin receptors (LH^{LEPR}) specifically drives appetitive behaviors in mice. Ablation of LH GABAergic neurons (LH^{VGAT}) decreases weight gain and food intake, whereas LH^{LEPR} ablation does not. Appetitive learning in a Pavlovian conditioning paradigm is delayed in LH^{VGAT}-ablated mice but prevented entirely in LH^{LEPR}-ablated mice. Both LH^{VGAT} and LH^{LEPR} neurons bidirectionally modulate reward-related behaviors, but only LH^{VGAT} neurons affect feeding. In the Pavlovian paradigm, only LH^{LEPR} activity discriminates between conditioned cues. Optogenetic activation or inhibition of either population in this task disrupts discrimination. However, manipulations of LH^{LEPR}→VTA projections evoke divergent effects on responding. Unlike food-oriented learning, chemogenetic inhibition of LH^{LEPR} neurons does not alter cocaine-conditioned place preference but attenuates cocaine sensitization. Thus, LH^{LEPR} neurons may specifically regulate appetitive behaviors toward non-drug reinforcers.

Graphical Abstract

This is an open access article under the CC BY-NC-ND license (<http://creativecommons.org/licenses/by-nc-nd/4.0/>).

*Correspondence: yeka.aponte@nih.gov.

AUTHOR CONTRIBUTIONS

J.N.S. and Y.A. designed the study. J.N.S., M.A.A., S.S., C.B.B., and C.N.R. performed the behavioral experiments, surgeries, and histology. J.N.S. and Y.A. analyzed the data and wrote the manuscript. All of the authors edited and approved the manuscript.

DECLARATION OF INTERESTS

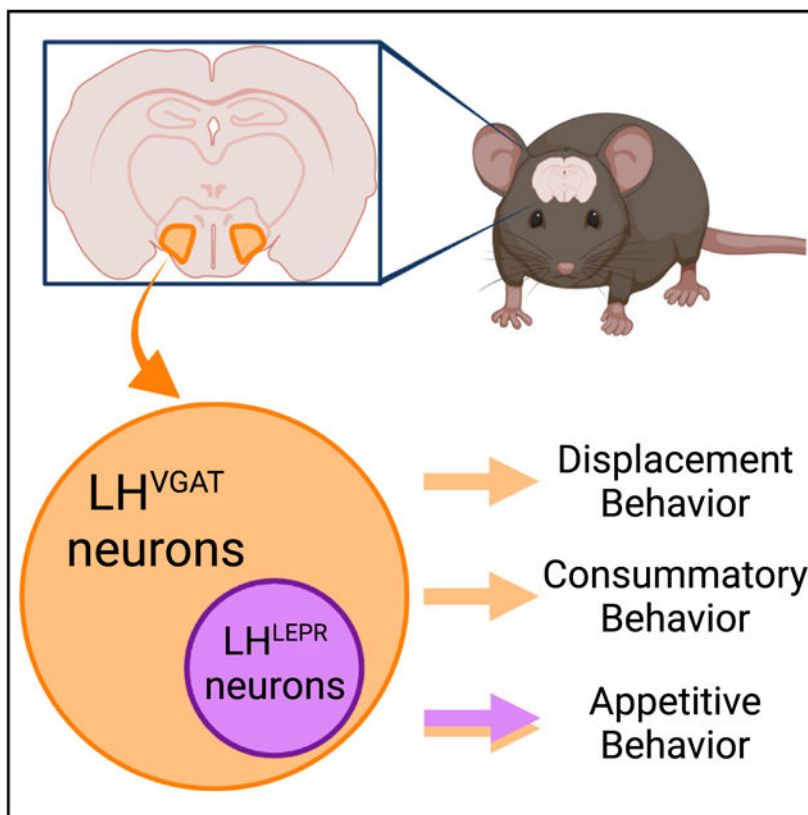
The authors declare no competing interests.

SUPPORTING CITATIONS

The following reference appears in the supplemental information: Saunders et al., 2012.

SUPPLEMENTAL INFORMATION

Supplemental information can be found online at <https://doi.org/10.1016/j.celrep.2021.109615>.



In brief

Siemian et al. investigate the functional contributions of leptin receptor-expressing lateral hypothalamic (LH^{LEPR}) neurons to the broader population of GABAergic LH (LH^{VGAT}) neurons in mice. They show that LH^{LEPR} neurons specifically mediate appetitive behaviors, whereas LH^{VGAT} neurons affect appetitive, consummatory, and displacement behaviors.

INTRODUCTION

The functional range of the lateral hypothalamus (LH) is likely due to its diverse cellular composition (Bonnayon et al., 2016; Brown et al., 2015; Stuber and Wise, 2016), and recent technological advances have begun to allow their detailed characterization. LH GABAergic (LH^{VGAT}) and glutamatergic (LH^{VGLUT2}) neurons have been revealed as opposing modulators of feeding and motivated behaviors (Jennings et al., 2013, 2015; Navarro et al., 2016; Nieh et al., 2016a; Qualls-Creekmore et al., 2017). However, LH^{VGAT} and LH^{VGLUT2} neurons are heterogeneous (Mickelsen et al., 2019), and it is likely that molecularly defined subgroups of neurons contribute to discrete aspects of behavior. *In vivo* calcium imaging experiments support this idea, as predominantly non-overlapping populations of LH^{VGAT} neurons were associated with either appetitive or consummatory behaviors (Jennings et al., 2015). However, the identities of these populations have not been elucidated.

To determine whether LH^{VGAT} subpopulations contribute differentially to appetitive or consummatory behaviors, we examined LH leptin receptor-expressing (LH^{LEPR}) neurons, which comprise ~20% of LH^{VGAT} cells (Schiffino et al., 2019). We previously showed that LH^{LEPR} activity bidirectionally affected food motivation via axonal projections in the ventral tegmental area (VTA) (Schiffino et al., 2019). The effects of leptin on LH^{LEPR} neurons have been implicated in food-directed behavior (de Vrind et al., 2019; Leininger et al., 2009, 2011), but leptin exerts heterogeneous effects on LH^{LEPR} neuronal activity (Leininger et al., 2009, 2011). Thus, intra-LH leptin administration does not characterize the roles of these neurons in behavior. Here, we directly compare the functions of LH^{LEPR} and LH^{VGAT} neurons in a range of tasks designed to assess consummatory and appetitive behaviors.

RESULTS

Targeted ablation of LH^{LEPR} neurons decreases appetitive but not consummatory behaviors

We compared behavioral effects after ablating LH^{VGAT} neurons or the LH^{LEPR} subpopulation. We bilaterally injected viruses expressing yellow fluorescent protein (YFP) or taCasp3 (Yang et al., 2013) into the LH of *Slc32a1^{Cre}* (LH^{VGAT}:YFP, LH^{VGAT}:taCasp3) or *Lepr^{Cre}* mice (LH^{LEPR}:YFP, LH^{LEPR}:taCasp3) (Figure 1A). Validation experiments similar to those performed by others (Tooley et al., 2018; Zhang and van den Pol, 2017) showed that taCasp3 injections substantially reduced LH^{VGAT} and LH^{LEPR} tdTomato⁺ neurons (Figures 1B, 1C, and S1). LH^{VGAT} ablation significantly attenuated weight gain (Figure 1D) and daily food intake (Figure 1E), whereas LH^{LEPR} ablation did not (Figures 1G and 1H). In a free-access feeding assay, LH^{VGAT}: taCasp3 mice performed fewer lick responses compared to control mice, whereas the lick responses of LH^{LEPR}:taCasp3 and LH^{LEPR}:YFP mice were similar (Figures 1F and 1I). Thus, LH^{LEPR} ablation does not appear to affect food intake.

We next examined whether LH^{VGAT} or LH^{LEPR} ablation modulates appetitive learning. We trained mice in a Pavlovian conditioning paradigm in which one auditory cue (CS⁺) preceded sucrose pellets, while a different auditory cue (CS⁻) had no outcome (Sharpe et al., 2017; Figure 1J). Time spent at the food port was monitored to assess conditioned responding during cues. Both LH^{VGAT}:YFP and LH^{VGAT}:taCasp3 mice learned to discriminate the CS⁺ and CS⁻ (Figure 1K), although the learning of LH^{VGAT}:taCasp3 mice was delayed (Figure 1K). Interestingly, LH^{LEPR}:taCasp3 mice exhibited greater deficits and did not learn to distinguish between cues (Figure 1M). Importantly, these learning impairments did not result from failure to collect and consume the sucrose pellets (Figures 1L and 1N). Thus, LH^{LEPR} cells are necessary for appetitive learning.

We last examined the effects of neuronal ablation on locomotion and displacement/anxiety-like behaviors (de Vrind et al., 2019; Qualls-Creekmore et al., 2017; Figure S1). LH^{VGAT} but not LH^{LEPR} ablation induced behavioral changes, and thus LH^{LEPR} neurons appear to be specifically involved in appetitive behaviors.

Optogenetic activation of LH^{LEPR} neurons does not evoke food intake but is rewarding

We next used optogenetics to acutely manipulate the activity of LH^{VGAT} or LH^{LEPR} neurons during feeding and reward-related tasks (Figure 2A), since adaptive mechanisms may compensate for genetic ablation and mask phenotypic changes (El-Brolosy and Stainier, 2017; Housden et al., 2017). For this, we bilaterally injected a virus expressing channelrhodopsin (ChR2), halorhodopsin (NpHR), or GFP (control) into the LH of *Slc32a1^{Cre}* or *Lep^{rCre}* mice and implanted optical fibers above the LH (Figures 2A–2C). Consistent with previous studies (Jennings et al., 2015), activation and inhibition of LH^{VGAT} neurons significantly increased and decreased food intake, respectively (Figures 2D and 2E), while manipulations of LH^{LEPR} activity did not (Figures 2F and 2G). We also tested whether LH^{VGAT} or LH^{LEPR} neurons affect reward or aversion with a real-time place preference (RTPP) assay (Figure 2A). As reported previously (Giardino et al., 2018; Jennings et al., 2015), both LH^{VGAT}:ChR2 and LH^{LEPR}:ChR2 mice displayed significant photostimulation-side preference relative to controls (Figures 2H and 2J), whereas both LH^{VGAT}:NpHR and LH^{LEPR}:NpHR mice spent significantly less time in the photoinhibition side compared to controls (Figures 2I and 2K). LH^{LEPR} activation also evoked frequency-dependent operant self-stimulation (Figure S2). These results demonstrate that LH^{LEPR} neurons contribute to the effects of the broader LH^{VGAT} population on appetitive-related behaviors but not food intake.

LH^{LEPR} but not LH^{VGAT} neurons discriminate reward-predictive from non-predictive cues

To investigate whether the activity of LH^{LEPR} neurons would reflect their differential involvement in appetitive over consummatory behavior in a task that included both aspects, we used *in vivo* imaging to measure the activity of LH^{VGAT} and LH^{LEPR} neurons during the Pavlovian paradigm. *Slc32a1^{Cre}* or *Lep^{rCre}* mice were injected in the LH with a virus expressing GCaMP6f. A gradient-index (GRIN) lens implanted above the LH was interfaced with a single-photon miniscope for the detection of GCaMP fluorescence (Figures 3A and 3B). Using MIN1PIPE (Lu et al., 2018), we extracted calcium traces from individual LH^{VGAT} or LH^{LEPR} neurons during behavioral testing. In a variant of the Pavlovian task, mice were conditioned to associate an auditory cue (CS⁺) with an Ensure droplet and a different auditory cue (CS⁻) with no reward. After training, we monitored Ca²⁺ dynamics in LH^{VGAT} or LH^{LEPR} neurons during one test session in which both groups of mice displayed >50% lick discrimination during the reward period on CS⁺ over CS⁻ trials (Figure 3C). Normalized activity of individual LH^{VGAT} neurons was plotted for both trial types (Figure 3D), and cells were grouped according to the epoch of CS⁺ trials in which they were maximally active: pre-cue, cue, or reward (Figures 3E–3G). This was repeated for LH^{LEPR} neurons (Figures 3H–3K). Activity of the epoch-selective groups of neurons was similar between genotypes, except for the cue-responsive neurons; LH^{LEPR} neurons appeared to discriminate between trial types and LH^{VGAT} neurons did not (Figures 3F and 3J). Comparison of the greatest group-maximum change from baseline on CS⁺ trials suggested that the effect of trial type on neuronal activity was dependent on genotype (Figure 3L). Lastly, we plotted the peak amplitude of all cue-responsive LH^{VGAT} and LH^{LEPR} neurons observed during the cue period on CS⁺ and CS⁻ trials without matching the sampled time bin across trials to assess the possibility that the maximum activity of individual LH^{LEPR} neurons on CS⁻ trials was comparable to CS⁺ trials but simply occurred

asynchronously across neurons or that individual LH^{VGAT} neurons discriminate between trial types by modulating their temporal dynamics. While the maximum activity of LH^{VGAT} neurons displayed a broad distribution of selectivity for CS⁺ and CS⁻ trials (Figure 3M), LH^{LEPR} neurons exhibited a distribution skewed toward greater CS⁺ selectivity (Figure 3N), which was confirmed by statistical comparison (Figure 3O). Thus, within the population of LH^{VGAT} neurons that positively respond to salient environmental stimuli, LH^{LEPR} cells are one specific subpopulation that discriminates between reward-predictive and non-predictive cues.

LH^{LEPR} neurons mediate appetitive learning via projections to the VTA

We next examined the effects of optogenetic activation or inhibition of each LH population during the appetitive learning task. During the Pavlovian conditioning task, photostimulation or photoinhibition was delivered concurrently with both auditory cues—the CS⁺ paired with sucrose pellets and the CS⁻ without pellets (Figure 4A). Photostimulation at 20 Hz was chosen as it is commonly used for LH stimulation (Jennings et al., 2015), and *in vivo* electrophysiological recordings demonstrated that most LH neurons did not surpass 20-Hz firing in a sucrose-seeking task (Nieh et al., 2015). An extinction test then occurred in which each cue was presented once without photomanipulation or pellets to assess how appetitive behavior developed (Figure 4A).

Across conditioning, LH^{VGAT}:GFP mice learned to discriminate the CS⁺ and CS⁻; however, discrimination was not observed in LH^{VGAT}:ChR2 mice or LH^{VGAT}:NpHR mice (Figure 4B), suggesting that both activation and inhibition of LH^{VGAT} cells disrupts the discrimination between auditory cues. Importantly, no significant differences in responding during sucrose delivery on CS⁺ trials were observed across groups (Figure 4C). The learning impairments in LH^{VGAT}:ChR2 and LH^{VGAT}:NpHR mice across conditioning did not affect cue discrimination on the subsequent extinction trial (Figure 4D). Similarly, we observed that LH^{LEPR}:GFP mice learned to discriminate the CS⁺ and CS⁻; however, discrimination was not observed in LH^{LEPR}:ChR2 or LH^{LEPR}:NpHR mice (Figure 4E), despite normal food port entry on pellet delivery (Figure 4F). Learning impairments did not persist to subsequent extinction trials for LH^{LEPR}:ChR2 or LH^{LEPR}:NpHR mice (Figure 4G). These results suggest that acute optogenetic manipulations of LH^{VGAT} or LH^{LEPR} neurons disrupt appetitive responding but do not affect overall task acquisition.

Since both LH^{VGAT} and LH^{LEPR} neurons project to the VTA (Nieh et al., 2015, 2016a; Schiffino et al., 2019; Sharpe et al., 2017), we examined whether this pathway drives appetitive learning as shown for GABAergic LH neurons in rats (Sharpe et al., 2017). For this, we injected ChR2, ArchT (archaerhodopsin), or GFP into the LH of *Slc32a1^{Cre}* or *Lepr^{Cre}* mice, but implanted optical fibers bilaterally above the VTA (Figures 4A and S3A). LH^{VGAT}:GFP→VTA mice learned to discriminate the CS⁺ and CS⁻. No significant discrimination between cues was observed in LH^{VGAT}:ChR2→VTA or LH^{VGAT}:ArchT→VTA mice (Figure 4H), despite normal food port entry following pellet delivery (Figure 4I). However, the learning impairments in both LH^{VGAT}:ChR2→VTA and LH^{VGAT}:ArchT→VTA mice across conditioning sessions did not persist in the extinction trial (Figure 4J). Lastly, LH^{LEPR}:GFP→VTA mice learned to discriminate the CS⁺ and

CS⁻ (Figure 4K). While no discrimination was observed in LH^{LEPR}:ChR2→VTA mice, LH^{LEPR}:ArchT→VTA mice displayed normal conditioned responding (Figure 4K), and each group exhibited normal food port entry following pellet delivery (Figure 4L). Strikingly, the learning effects in LH^{LEPR}:ChR2→VTA and LH^{LEPR}:ArchT→VTA mice were reflected in the subsequent extinction trial (Figure 4M). Thus, optogenetic manipulations of LH^{LEPR} axonal projections to the VTA during conditioning impart persistent effects on appetitive responding and affect overall acquisition of the task. Importantly, no significant differences in food cup responding during the pre-CS period were observed across cohorts (Figures S3B–S3E), and none of the optogenetic manipulations in any cohort altered locomotion (Figures S3F–S3I).

LH^{LEPR} neurons regulate sucrose-context but not cocaine-context learning

We last examined whether LH^{LEPR} neuron involvement in appetitive behavior generalized to both drug and non-drug reinforcers. For this, we compared the effects of manipulating LH^{LEPR} activity between sucrose- and cocaine-conditioned place preference (CPP), a Pavlovian learning model depending on learned associations with the stimulus-paired context (Cunningham et al., 2006). We used chemogenetics to manipulate activity throughout conditioning sessions (Allen et al., 2015; Schiffino et al., 2019) by injecting viruses expressing the excitatory hM3D, inhibitory hM4D, or mCherry (control) into the LH of *Lepr^{Cre}* mice (Figures 5A and 5B). For sucrose CPP (Figure S4A), all of the groups exhibited a comparable pre-test side bias (Figure 5C). In alternating location-restricted training sessions, one side contained an offering of sucrose pellets, while the other side contained cellulose pellets. Clozapine-*N*-oxide (CNO) was administered 1 h before sucrose conditioning sessions. No changes in side preference were observed during an intermediate test session in any group (Figure 5C, post 1), so mice were conditioned for an additional 8 sessions with an increased offer of 100 sucrose pellets during sucrose conditioning sessions. A second post-test revealed that LH^{LEPR}:mCherry and LH^{LEPR}:hM3D mice displayed significantly increased preference to the sucrose-paired side, whereas LH^{LEPR}:hM4D mice did not (Figure 5C, post 2). No between-group differences in sucrose intake were observed during either phase (Figure 5D). Thus, LH^{LEPR} inhibition impairs the appetitive context association normally formed during sucrose consumption without affecting consummatory behavior.

Since sucrose CPP was unaffected in LH^{LEPR}:hM3D mice, we next studied only the effects of LH^{LEPR} inhibition on the acquisition of cocaine CPP in a new cohort of mice (Figure S4B). Following a pre-test session, one side was paired with cocaine and the other side was paired with saline in alternating training sessions, and CNO was administered 1 h before cocaine. LH^{LEPR} inhibition during this training did not affect context preference when measured in a subsequent free-choice session, indicating normal formation of the cocaine-context association (Figure 5E). We then extinguished place preference and reinstated with another injection of cocaine, a procedure shown to reflect the persisting drug-context association (Itzhak and Martin, 2002; Steketee and Kalivas, 2011). However, LH^{LEPR}:hM4D mice displayed significant cocaine-induced reinstatement similar to controls (Figure 5E). This null effect of LH^{LEPR} inhibition on the response to cocaine was likely specific to associative learning, as it significantly attenuated the development of cocaine-induced

locomotor sensitization in a separate group of mice. No effects of CNO pretreatment on the acute locomotor effects of cocaine in wild-type mice were observed (Figures S4C and S4D; Gomez et al., 2017; MacLaren et al., 2016). While LH^{LEPR} inhibition did not alter open field locomotion (Figures S4E and S4F) or acute locomotor responses to cocaine (Figure 5F), it did significantly attenuate the gradual daily increases in cocaine-induced locomotion (Figure 5G). This was also reflected in cocaine challenge sessions without acute LH^{LEPR} inhibition conducted after short- (Figure 5H) and long-term (Figure 5I) cocaine abstinence. Thus, LH^{LEPR} neurons may only alter appetitive learning about non-drug reinforcers.

DISCUSSION

Our study implicates LH^{LEPR} neurons specifically in the regulation of appetitive behaviors, in contrast to the broad LH^{VGAT} population. Intra-LH leptin administration was previously shown to decrease food intake but heterogeneously affect LH^{LEPR} activity (Leininger et al., 2009), and thus did not describe the role of these neurons from a systems neuroscience perspective. Our gain- or loss-of-function manipulations of LH^{LEPR} activity never affected food intake, locomotion, or displacement/anxiety-like behaviors. Instead, these cells only affected appetitive behaviors, namely RTPP and appetitive associations to food-paired cues. These findings broadly agree with those of previous studies of molecularly defined subpopulations of LH^{LEPR} neurons, including galanin⁺ and neurotensin⁺ LH^{LEPR} neurons, manipulations of which had greater effects on motivation and appetitive behavior rather than food intake (Brown et al., 2019; Laque et al., 2015; Leininger et al., 2011). Thus, although LH^{LEPR} neurons are molecularly heterogeneous (Mickelsen et al., 2019), they nonetheless specifically regulate appetitive behaviors. Photostimulation frequency or location within the LH were previously able to untangle LH-associated feeding and reward (Barbano et al., 2016; Urstadt and Berridge, 2020), but our study now deconstructs these processes on a genetic basis.

Using *in vivo* imaging, we revealed that LH^{VGAT} and LH^{LEPR} neurons respond to learned reward-predictive and non-predictive cues. While subgroups of both LH^{VGAT} and LH^{LEPR} neurons displayed maximal activity during the CS⁺, divergent activity on CS⁻ trials was only observed for LH^{LEPR} neurons that may be critical for behavioral discrimination between cues. Other subgroups within the broader LH^{VGAT} population may not discriminate between trial types or respond selectively to the CS⁻ to produce the lack of activity discrimination within this broad neuronal population. While the activity of both populations was also increased post-CS⁺ relative to post-CS⁻, this may, at least for LH^{LEPR} neurons, reflect outcome evaluation as opposed to food consumption, since gain- and loss-of-function manipulations of LH^{LEPR} activity did not affect consummatory behavior.

Our results using optogenetics during Pavlovian conditioning are unique from a previous study in rats (Sharpe et al., 2017), as the apparent learning decrements associated with somatic LH manipulations during training were not later reflected during extinction trials, suggesting the acute manipulations interfered with appetitive responding but not learning per se. Coupled with previous findings that the inhibition of GABAergic LH neurons attenuated responding to appetitive cues in well-trained rats (Sharpe et al., 2017), the acute activity of LH^{VGAT} and LH^{LEPR} neurons seems both necessary and sufficient for

discrimination between conditioned stimuli. That is, artificially matching neuronal activity via optogenetics across trial types caused behavioral generalization between cues. However, since the optogenetic manipulations were only applied during the cue period and not the outcome, the spontaneous activity during reward delivery/outcome evaluation observed via functional imaging may be sufficient to drive appropriate behavior during CS trials without optogenetic manipulation in extinction. Our results from the caspase ablation experiments support this possibility, as the temporally non-specific removal of LH^{VGAT} or LH^{LEPR} activity evoked more pronounced deficiencies in appetitive learning.

Learning theory predicts that during early learning, large differences between expectations and outcomes evoke proportionally large error signals, reflected in neurophysiology as VTA dopamine prediction errors (Rescorla and Wagner, 1972; Schultz et al., 1997). Across training, expectations more closely match outcomes, and the size of dopamine error signals attenuates. Inhibiting LH GABAergic axonal projections in the VTA during Pavlovian conditioning was previously shown to enhance learning in rats (Sharpe et al., 2017). These LH neurons likely transmit information to the VTA about the size of the expected reward. Inhibiting this transmission likely prevents the accommodation of dopamine error signals, causing them to be continuously oversized and the asymptote of learned associations to surpass usual limits (Sharpe et al., 2017). Conversely, activating this pathway during training should cause dopamine errors to be continuously undersized, slowing the rate and decreasing the strength of learned associations. Here, while LH^{VGAT}→VTA manipulations did not affect learning, LH^{LEPR}→VTA inhibition increased discrimination between the cues during training and extinction. Accordingly, activation of this pathway abolished discrimination during training and extinction. These results implicate the LH^{LEPR}→VTA pathway not only in modifying acute appetitive responses but also in regulating the overall acquisition of learned appetitive behavior. Since LH^{LEPR} cells synapse primarily with non-dopaminergic VTA neurons (Schiffino et al., 2019), the modified learning in the present study was likely due to altered timing and/or magnitude of dopamine error signals in line with the above theory (Sharpe et al., 2017). While it is unclear why the broader LH^{VGAT}→VTA manipulation did not evoke similar effects, it is not likely due to ArchT-mediated presynaptic release (Mahn et al., 2016), as this issue has not arisen *in vivo* (Jennings et al., 2013; Rozeske et al., 2018). Furthermore, these results echo our genetic ablation data, in which Pavlovian appetitive responding was more affected in LH^{LEPR}-ablated than LH^{VGAT}-ablated mice. However, one limitation of this study was validating the neuronal ablation method. While we demonstrated that the caspase virus robustly ablated the targeted LH neurons, different subjects that did not undergo post-mortem cell death quantification were used in the behavioral experiments. Therefore, all of the subjects were included from the experimental cohorts, which seemed a low-bias approach. Adjacent hypothalamic regions also express LEPR and VGAT, and affecting these regions via off-target injections may have also contributed to behavioral changes. Nevertheless, the similarity of observations across other more easily validated approaches such as optogenetics, chemogenetics, and calcium imaging generally support the findings from the caspase experiments.

The finding that LH^{LEPR} inhibition decreased sucrose yet did not affect cocaine CPP, suggests that LH^{LEPR} neurons specifically regulate non-drug learning. However, LH^{LEPR}

activity does appear critical to some cocaine-mediated behavioral effects, as inhibition significantly decreased the development of cocaine-induced locomotor sensitization, suggesting that cocaine does not simply bypass or override the effects of the LH manipulations used in this study. Clearly, further investigations are still needed to clarify the role of LH^{LEPR} neurons in drug-related behaviors. Thus, our work specifically implicates LH^{LEPR} neurons in the regulation of non-drug-associated appetitive behaviors and will serve as a framework for future studies to distinguish the contributions of neuronal subpopulations to behavior.

STAR★METHODS

RESOURCE AVAILABILITY

Lead contact—Further information and requests for resources and reagents should be directed to and will be fulfilled by the Lead Contact, Yeka Aponte (yeka.aponte@nih.gov).

Materials availability—This study did not generate new unique reagents.

Data and code availability

- All data reported in this paper will be shared by the lead contact upon request.
- This paper does not report original code.
- Any additional information required to reanalyze the data reported in this paper is available from the lead contact upon request.

EXPERIMENTAL MODEL AND SUBJECT DETAILS

Animals—All experimental protocols were conducted in accordance with U.S. National Institutes of Health Guidelines for the Care and Use of Laboratory Animals and with the approval of the National Institute on Drug Abuse Animal Care and Use Committee. Male and female heterozygous *Lepr^{Cre}* (*Lepr^{tm3(cre)Mgmj}*; C57BL/6J background; kindly provided by M.G. Myers Jr., University of Michigan Medical School, MI, USA) (Leshan et al., 2006), *Lepr^{Cre/+};Rosa26^{YFP/YFP}* mice (*Lepr^{Cre}* crossed to *Gt(ROSA)26Sor^{tm3(CAG-EYFP)Hze}*; C57BL/6J background; Strain 7903, The Jackson Laboratory, ME, USA), or heterozygous *Slc32a1^{Cre}* (*Slc32a1^{tm2(cre)Low1}*; C57BL/6J background; Strain 28862, The Jackson Laboratory) mice were used in this study. Mice were maintained at the National Institute on Drug Abuse Intramural Research Program animal facility under standard housing conditions. Up to five mice of the same sex were group housed under a 12-hour light-dark cycle at 20 – 24°C and 40 – 60% humidity with free access to water and food (PicoLab Rodent Diet 20, 5053 tablet, LabDiet/Land O'Lakes Inc., MO, USA). For behavioral experiments, six- to eight-week-old male and female mice (~18 – 25 g) were randomly assigned to experimental groups while maintaining littermate or age-matched and gender-matched controls. Following stereotaxic surgeries, mice were individually housed.

METHOD DETAILS

Surgical procedures—For behavioral experiments, mice were anesthetized with isoflurane and placed onto a stereotaxic apparatus (David Kopf Instruments, CA, USA).

After exposing the skull by a minor incision, small holes (< 1-mm diameter) were drilled bilaterally for virus injection. For all experiments, 40 – 50 nL of an adeno-associated virus was injected bilaterally (rate: 30 nl/min) into the LH (bregma: –0.90 to –1.50 mm; midline: \pm 1.10 mm; dorsal skull surface: –4.75 to –5.20 mm) by a pulled glass pipette (20 – 30 μ m tip diameter) with a micromanipulator (Narishige International USA Inc., NY, USA) controlling the injection speed. Viruses injected include the following:

1. rAAV2/1-EF1 α -FLEX-taCasp3-TEVp, titer: 1.9×10^{12} GC/ml, Addgene 45580, University of North Carolina (UNC) Vector Core (NC, USA) viral prep;
2. rAAV2/1-EF1 α -DIO-YFP, titer: 1.9×10^{12} GC/ml, Addgene 27056, Addgene (MA, USA) 27056-AAV9 viral prep;
3. rAAV2/1-CAG-FLEX-tdTomato, titer: 2.0×10^{13} GC/ml, Addgene 51503, Addgene 51503-AAV1 viral prep;
4. rAAV2/1-CAG-FLEX-rev-ChR2-tdTomato, titer: 6.8×10^{12} GC/ml, Addgene 18917, University of Pennsylvania (Penn) Vector Core (PA, USA) viral prep;
5. rAAV2/9-CAG-FLEX-tdTomato, titer: 4.1×10^{13} GC/ml, Addgene 51503, Penn Vector Core viral prep;
6. rAAV2/5-EF1 α -DIO-eNpHR3.0-eYFP, titer: 6×10^{12} GC/ml, Addgene 26966, UNC Vector Core viral prep;
7. rAAV2/9-CAG-FLEX-ArchT-GFP, titer: 4.7×10^{12} GC/ml, Addgene 28307, UNC Vector Core viral prep;
8. rAAV2/9-CAG-FLEX-GFP, titer: 2.3×10^{12} GC/ml, Addgene 51502, Addgene 51502-AAV9 viral prep;
9. rAAV2/9-hSyn-DIO-hM3D(Gq)-mCherry, titer: 5.0×10^{12} GC/ml, Addgene 44361, Addgene 44361-AAV9 viral prep (Krashes et al., 2011);
10. rAAV2/9-hSyn-DIO-hM4D(Gi)-mCherry, titer: 5.0×10^{12} GC/ml, Addgene 44362, Addgene 44362-AAV9 viral prep (Krashes et al., 2011);
11. rAAV2/9-hSyn-DIO-mCherry, titer: 5.0×10^{12} GC/ml, Addgene 50459, Addgene 50459-AAV9 viral prep.

For caspase experiments, separate mice were used for virus validation than for behavioral experiments. To estimate the amount of neuronal ablation achieved by transduction of the taCasp3 virus, mice used for validation were injected in one LH hemisphere with a cocktail of 10 parts rAAV2/1-EF1 α -FLEX-taCasp3-TEVp to 1 part rAAV2/1-CAG-FLEX-tdTomato (final titers of 1.73×10^{12} and 1.82×10^{12} GC/ml, respectively) and in the other LH hemisphere with 10 parts sterile PBS to 1 part rAAV2/1-CAG-FLEX-tdTomato (Oh et al., 2014). After 30 days, mice were euthanized, and tissue was analyzed. Briefly, 500 μ m \times 500 μ m square ROIs were positioned at LH injection sites and tdTomato-positive cells were counted.

For optogenetic experiments targeting LH neuronal soma, optical fibers were implanted bilaterally at 10° angles above the LH (bregma: –0.90 to –1.50 mm; midline: \pm 1.80

mm; dorsal skull surface: -4.50 mm). For optogenetic experiments targeting LH axonal projections within the VTA, optical fibers were implanted bilaterally at 10° angles above the VTA (bregma: -3.0 mm; midline: ± 1.12 mm; skull surface: -4.10 mm). Fiber implants were affixed to the skull with cyanoacrylate adhesive and C&B Metabond Quick Adhesive Cement System (Parkell, Inc., NY, USA). Subsequently, mice were individually housed for four weeks for post-surgical recovery and viral transduction.

For *in vivo* functional imaging experiments, mice were anesthetized with isoflurane and placed onto a stereotaxic apparatus (David Kopf Instruments). After exposing the skull by a minor incision, a small hole (< 1 -mm diameter) was drilled unilaterally (bregma, -1.55 mm; midline, $+0.95$ mm) for virus injection and GRIN lens insertion. A sterile, beveled 25-gauge needle was inserted into the center of the craniotomy stopping approximately 50 μm above the dorsal-ventral coordinate for the lens implant to avoid damaging the field of view and remaining in place for 4 – 5 min to prepare a path for the implant. Next, rAAV2/9-CAG-FLEX-GCaMP6f-WPRE-SV40 (Chen et al., 2013) was injected 150 μm offset from the center of the craniotomy (150 nl; rate: 25 nl/min; titer: 5.0×10^{12} GC/ml; Addgene 100835, Addgene viral prep 100835-AAV9) into the LH of *Lep1^{Cre}* or *Slc32a1^{Cre}* mice (bregma, -1.55 mm; midline, $+0.70$ mm; skull surface, -5.40 mm) by a pulled glass pipette (20 – 30 μm tip diameter) with a micromanipulator (Narishige International USA Inc.) controlling the injection speed. After injection, a 500 - μm -diameter GRIN lens (Snap-in Imaging Cannula Model L-V; Doric Lenses, Inc., Québec, QC, Canada) was lowered into the center of the craniotomy (bregma, -1.55 mm; midline, $+0.95$ mm; skull surface, -5.25 mm). Implants were affixed to the skull with C&B Metabond Quick Adhesive Cement System (Parkell, Inc.). Subsequently, mice were individually housed for three to four weeks for post-surgical recovery and viral transduction.

Optical manipulations—Optical fiber implants were coupled to patch cords which were connected to lasers (Doric Lenses Inc., Quebec, Canada) via rotary joints mounted over behavioral testing areas. Laser output was controlled by Doric Neuroscience Studio software (v5.1). For photostimulation experiments, 450-nm laser diodes were used to deliver 5-ms pulses of 10- to 15-mW light at a frequency of 20 Hz. For photoinhibition experiments, 520-nm laser diodes were used to deliver 10 – 15 mW of constant light.

Behavioral experiments—Mice were handled for 3 days prior to testing to habituate them to the experimenter, and all experiments were performed during the light cycle. Mice were acclimated to behavioral rooms for at least 1 h before experiments began. Across experimental and control groups, mice were gender-matched and age-matched or littermates. Mice were excluded from analysis if viral expression and fiber placement were not observed in at least one hemisphere after histological assessment (see Histology).

Home cage observations—Bodyweight was measured daily following surgery for mice in caspase-induced genetic ablation experiments. Beginning 7 days post-surgery, the daily home cage food intake of these mice was measured by subtracting the weight of the food in the hopper from the previous day's food weight.

Free-access liquid consummatory assay—Beginning after day 30 post-surgery, *ad libitum*-fed mice in caspase-induced genetic ablation experiments were habituated to test cages with fluid spouts equipped with lickometers. After 3 daily 1-h habituation sessions to a spout filled with water, a 1-h test session was conducted in which a caloric liquid (vanilla Ensure; Abbott Laboratories, IL, USA) was freely available and the total number of licks was recorded.

Open field test—Open field tests for caspase ablation studies were conducted in 30 × 30 cm clear acrylic arenas housed inside sound-attenuating chambers. A thin layer of bedding was placed on the chamber floor, and diffuse lighting illuminated the chamber interior. Mice naive to the chambers were gently placed inside and the total locomotion and time spent in the center area of the open field over 1 h was measured with ANY-maze video tracking system v5 (Stoelting Co., IL, USA).

Marble burying test—Marble burying test procedures were used as previously described (Deacon, 2006). Standard mouse cages were filled with fresh bedding to a depth of 5 cm and 16 marbles were evenly spaced across the bedding in a 4 × 4 rectangular grid. At the end of the 30-min test period, the number of marbles buried was quantified as follows: 1 for marbles entirely covered with bedding, 0.5 for marbles with surfaces exposed but covered > 50% with bedding, and 0 for anything less (Shin Yim et al., 2017).

Free-access feeding with optogenetics—For photostimulation experiments, *ad libitum*-fed mice were placed into standard rat housing cages that were empty except for two plastic weigh boats secured to the floor in opposing corners of the cage. One weigh boat contained grain pellets of identical composition to the standard chow (PicoLab Rodent Diet 20), and the other contained cellulose pellets (5TUW; TestDiet, MO, USA). Mice were habituated to the food and cellulose pellets in their home cages for 3 days prior to testing. Tests were 1 h in duration and pellet consumption was assessed at the end of each of 3 consecutive 20-min epochs: pre-photostimulation, photostimulation, and post-photostimulation.

For photoinhibition experiments, food-restricted mice were habituated to the grain and cellulose pellets in their home cages for 3 days before the test. The test was performed with the same chambers and setup as described for photostimulation experiments, except four 10-min epochs were used. Photoinhibition was paired with the second and fourth epochs, and pellet consumption was assessed following each 10-min epoch.

For these tests, only consumption of grain pellets was reported. Cellulose pellets were occasionally observed to be chewed, but the weight of the pellets in the dish never changed by more than the weight of a single pellet (20 mg). Therefore, these data were not reported.

Real-time place preference (RTPP)—20-min RTPP sessions were performed in a standard rat cage with opaque black siding filled with a thin layer of clean rodent bedding. Freely fed mice were placed into the chamber, and photostimulation or photoinhibition was paired with one-half of the chamber's area, which remained constant across all tests. The same control cohort was used for both photostimulation and photoinhibition cohorts;

retesting was performed after 7 days to avoid context habituation. At the end of the sessions, the percentage of time spent on the laser-paired side was calculated by ANY-maze software.

Pavlovian conditioning—Training was conducted in standard mouse behavioral test cages (Coulbourn Instruments, Inc., PA, USA) individually housed within ventilated light- and sound-attenuating chambers. Each test cage had a pellet dispenser that delivered one 20-mg pellet into a recessed magazine when triggered. Access to the magazine was monitored by infrared detectors mounted above and below the opening of the port. Each chamber contained a seven-tone auditory stimulus generator (Coulbourn Instruments, Inc.), which delivered either a single clear tone (“tone”) or two rapidly alternating tones similar to the sound of a traditional phone ringtone (“phone”) when activated. Both stimuli were presented at 75 dB. Graphic State v4 software (Coulbourn Instruments, Inc.) was used to control the equipment and record the responses.

All conditioned stimuli were 10 s in duration, separated by a variable intertrial interval (ITI) with a mean of 4 min (range = 2 to 6 min). The two auditory stimuli described were used in these experiments; whether the “phone” or “tone” stimulus was the CS+ was counterbalanced across mice. The order of stimulus presentation in all behavioral sessions was randomized by Graphic State software with the constraint that each stimulus was presented six times.

Mice were first food-restricted to 90% of their baseline body weight and habituated to sucrose pellets (TestDiet 5TUT) in their home cage for 3 d. On the first day of behavioral training, mice learned to retrieve pellets from the food magazine. During this session, mice received fifteen 20-mg sucrose pellets across a 30-min period. After food port training, mice received nine (optogenetic experiments), twelve (CS+ photostimulation-only experiments (Figure S1A)), or fifteen (caspase experiments) conditioning sessions, each consisting of six presentations of each stimulus. During these sessions, termination of one of the cues was followed 1 s later by delivery of two sucrose pellets; this cue was designated the CS+. The other stimulus was presented alone without food and was designated the CS-. For optogenetic experiments, light was delivered into either the LH or VTA during both cue presentations during conditioning. Light delivery began 500 ms prior to cue onset and continued until 500 ms after cue presentation to ensure that cells were affected by light for the duration of the cue presentation. Following conditioning, mice in optogenetic experiments received a cue test where the CS+ and CS- were each presented once, without light or food delivery. For all training sessions, responding during the last 5 s of cue presentation (“Responding during CS”) and during the 2 s period beginning 1 s after cue termination (“Responding during reward”) are presented, with baseline responding (measured during the 10 s pre-CS periods, Figure S3) subtracted. Each training “block” plotted was generated by averaging responding across three daily sessions (Sherwood et al., 2012). For extinction sessions, responding during the last 5 s of cue presentation, with baseline responding subtracted, was plotted (“Responding during extinction”).

Optogenetic self-stimulation—LH^{LEPR}:ChR2 and LH^{LEPR}:tdTomato mice were trained in three daily 20-min sessions to lever press on a fixed ratio 1 (FR1) schedule for optogenetic self-stimulation in standard mouse operant chambers equipped with 1 lever.

Each lever press produced a 1 s, 20-Hz pulse train accompanied with a 1 s auditory cue (white noise; white noise generator, Coulbourn Instruments). Following these three training days, mice were given four daily 20-min test sessions in which lever presses evoked different photostimulus frequencies (40, 20, 10, and 5 Hz); tests were conducted in the order of decreasing photostimulus frequency. Mice were then food-restricted for 3 days (fed 2.5 to 3 g per day) and given the same four-test protocol to examine if feeding status altered the reinforcing properties of stimulating LH^{LEPR} neurons.

Locomotion with optogenetics—Following Pavlovian conditioning experiments, all mice from optogenetic cohorts were used for locomotor assays to examine whether changes in Pavlovian conditioning were due to locomotor impairment or facilitation. Mice were connected to patch cords and placed in open field chambers (dimensions: 30 cm × 27 cm × 30 cm) equipped with ANY-maze animal tracking systems (Stoelting Co.) for 30 min. Alternating 3-min epochs were paired with photostimulation or photoinhibition for 6 blocks each of ON-OFF or OFF-ON; the order was counterbalanced across mice. The total distance traveled in the ON epochs and the OFF epochs was calculated.

Conditioned place preference (CPP)—CPP experiments were performed in a two-chamber apparatus separated by a wall with a small door that could be closed with a divider. One chamber (“side A”) had a metal grid floor, walls decorated with tan and black alternating vertical stripes, and almond scent. The other chamber (“side B”) had a smooth white floor, walls decorated with white circles on a tan background, and orange scent. The front wall of each chamber remained clear, and sessions were recorded using video cameras aimed through this wall using ANY-maze software. The chambers were thoroughly cleaned between mice. Pilot experiments showed that mice consistently preferred side A at a rate of 60 – 70% per 15-min test. In comparison to using an unbiased design, this biased design enabled us to pre-assign groups at surgery with less potential for mismatched side preference at pre-test.

For sucrose CPP, following the pre-test session, mice received “phase 1 training,” consisting of one training session per day for eight days with the center door closed and only one chamber accessible; these sessions were not recorded. On even days (sessions 2, 4, 6, and 8), mice received an injection of saline and were immediately placed on side A for 30 min with access to ten 20-mg calorie-free, flavorless cellulose pellets (TestDiet 5TUV). On odd days (sessions 3, 5, 7, and 9), mice received a 1-h pretreatment with 1 mg/kg CNO (intraperitoneal, i.p.; Tocris Bioscience, Bristol, UK) and were placed on side B for 30 min with access to ten 20-mg sucrose pellets. Pellet consumption was recorded at the end of each session; cellulose pellets were rarely eaten, so these data were not shown. After these eight conditioning sessions, a 15-min post-test (“Post 1”) was performed. Mice then received “phase 2 training,” which was identical to phase 1 training except that sessions were conducted twice per day (once on side A and once on side B, alternating order) and that 100 sucrose pellets were offered during sucrose training sessions. After these eight conditioning sessions, a second 15-min post-test (“Post 2”) was performed.

For cocaine CPP, after the pre-test session, mice received one training session per day for eight days with the center door closed and only one chamber accessible; these sessions were

not recorded. On even days (sessions 2, 4, 6, and 8), mice received an injection of saline and were immediately placed on side A for 30 min. On odd days (sessions 3, 5, 7, and 9), mice received a 1-h pretreatment with 1 mg/kg CNO (i.p.) before being injected with 15 mg/kg cocaine hydrochloride (i.p.; National Institute on Drug Abuse Drug Supply Program, MD, USA) and placed on side B for 30 min. Both drugs were dissolved in 0.9% saline. On day 10, untreated mice were placed back in the testing arena with free access to both chambers and the sessions were analyzed with ANY-maze software. For CPP extinction, mice were placed into the apparatus with access to both chambers for twelve 30-min sessions, and then, a 15-min extinction test was performed to verify a decrease in group preference for the cocaine-paired side to under 50%. The next day, 15 mg/kg cocaine (i.p.) was injected immediately prior to placing the mice in the apparatus with free access to both chambers and the session was analyzed with ANY-maze software.

Locomotor sensitization—Locomotor sensitization experiments were conducted in 30 × 30 cm plexiglass chambers and ANY-maze software monitored mouse locomotor activity via a camera suspended above the behavioral arena. We initially tested whether CNO affected novel open field locomotion or cocaine-induced locomotion in wild-type mice (Gomez et al., 2017; MacLaren et al., 2016) by administering CNO (1 mg/kg, i.p.) 30 min before placing mice in the chambers for 30 min, then giving a second injection of cocaine (15 mg/kg, i.p.), and monitoring locomotion for another 60 min.

The protocol used for locomotor sensitization was adapted from an earlier study (Thorn et al., 2014). Briefly, LH^{LEPR}:mCherry and LH^{LEPR}:hM4D mice were initially assessed for changes in locomotor activity following a 60 min pretreatment with CNO (1 mg/kg, i.p.). Following two more days of 60-min habituation to the chambers, cocaine testing began. For dose-response curve tests, saline (1 ml/kg) was administered immediately prior to the start of the test session and doses of cocaine (cumulative doses of 3.2, 10, 32 mg/kg, i.p.) were given at 20 min, 40 min and 60 min. The locomotor effects of each dose of cocaine were recorded for 20 min, but the first 5 min immediately following each injection were discarded because mice demonstrate a brief hyperactivity due to handling and injection. This procedure generates highly consistent and reliable dose response curves of drugs such as morphine, cocaine and methamphetamine (Baladi et al., 2012; Li et al., 2013; McGuire et al., 2011). For the first cocaine dose-response curve on day 1, mice were given an injection of CNO (1 mg/kg, i.p.) 30 min prior to the test. On days 2 – 7, mice were given CNO (1 mg/kg, i.p.) 30 min prior to a single injection of 15 mg/kg cocaine (i.p.), after which, mice were placed in the chambers for 60 min; the first 30 min of each session were analyzed as they contained the majority of the locomotor activity. On day 8, mice were given a second cocaine dose-response curve test without CNO pretreatment. Mice were then given a 7-day forced abstinence period from cocaine and were left in their home cages undisturbed. On day 16, a third and final cocaine dose-response curve test without CNO pretreatment was conducted.

***In vivo* functional imaging**—A miniature microscope with an integrated LED was used to image GCaMP6f fluorescence in LH^{VGAT} and LH^{LEPR} neurons through an implanted GRIN lens (Basic Fluorescence Snap-In Microscopy System – Deep Brain; Doric Lenses,

Inc.). Mice were tethered to the microscope throughout training to become habituated to handling, microscope attachment, and microscope weight. The day of the imaging session, GRIN lenses were briefly cleaned with isopropanol and mice were gently restrained while the snap-in microscope was secured to the baseplate for alignment with the implanted GRIN lens. Mice were then given approximately 5 min to acclimate to the microscope and tether. Grayscale TIFF images were collected at 10 frames per second (100-ms exposure) using Doric Neuroscience Studio software version 5.1. The LED power was calibrated between 10% and 50% (0.2 – 1.2 mW of 458-nm blue light). At the beginning of the session, imaging was synchronized via TTL with GraphicState behavioral recording software (v4, Coulbourn) for later alignment.

Behavioral training was performed in the same apparatuses as described above for Pavlovian conditioning, but several adaptations were made. Mice were food-restricted to 90% of their free-feeding body weight for 3 day prior to the onset of training, which lasted 8 days before the imaging test session. Each session lasted 30 min and included 10 presentations of each CS presented in a pseudorandomized order and separated by a variable ITI. The CS+ was 5 s, and a droplet of highly palatable and caloric liquid food (vanilla Ensure) was dispensed across the final second. The CS– was 5 s, and no programmed consequence followed. A touch sensor attached to the sipper monitored lick events throughout the session, those occurring in the 4 s period 1 s before CS termination until 3 s after CS termination were analyzed for task engagement and performance.

Imaging and behavioral analysis—Image analyses were performed in MATLAB using the open source pipeline MIN1PIPE (Lu et al., 2018) (<https://github.com/JinghaoLu/MIN1PIPE>). A total of 198 neurons from 8 *Lepr^{Cre}* mice and 322 neurons from 9 *Slc32a1^{Cre}* mice were extracted. Time-locked traces surrounding each CS+ or CS– event (–3 s to +10 s) were collected from each extracted neural segment, and were then averaged, smoothed with a 10-frame moving window, and peak-normalized (baseline was considered the –3 s to 0 s period) within each CS to generate the normalized traces per stimulus per neuron. Neurons were grouped according to the epoch of CS+ trials in which they were maximally active: pre-cue, cue, or reward. The activity during the time on CS+ trials that displayed the greatest change from baseline per neuronal subset was used to collect data from both CS+ and CS– trials for a three-way ANOVA. The cue-responsive subset was further analyzed by collecting data from the time bin in which the greatest change from baseline occurred, without matching the time bin across trial types.

Histology—Mice were deeply anesthetized with isoflurane and transcardially perfused with 1x phosphate buffered saline (PBS) followed by 4% paraformaldehyde (PFA) in 1x PBS. Whole brains were removed and post-fixed in 4% PFA until further processing. Samples were cryoprotected in 30% sucrose in 11x PBS, frozen on dry ice, and mounted in Cryo-Gel Tissue Embedding Medium (Leica Biosystems GmbH, Wetzlar, Germany). Coronal brain sections (50 μ m thick) were collected in 1x PBS using a Leica Biosystems CM3050 S cryostat. Sections were mounted with DAPI-Fluoromount-G aqueous mounting medium (Electron Microscopy Sciences, PA, USA) onto Superfrost Plus glass slides (Fisher

Scientific, NH, USA). Images were taken with an AxioZoom.V16 fluorescence microscope (Carl Zeiss Microscopy LLC, NY, USA).

QUANTIFICATION AND STATISTICAL ANALYSIS

Graphs and statistics were generated with GraphPad Prism 8 software (GraphPad Software, CA, USA). All data are plotted as mean \pm SEM. Data were analyzed with paired or unpaired Student's t tests, linear regression, or one-, two-, or three-way repeated-measures or mixed-model ANOVAs as indicated in the figure legends and/or Table S1. Group sizes and full statistics are indicated in Table S1. Data distributions were assumed to be normal. Sample sizes were chosen based on similar prior experiments (Jennings et al., 2015; Schiffino et al., 2019; Sharpe et al., 2017) which have yielded significant results with similar numbers of mice.

Supplementary Material

Refer to Web version on PubMed Central for supplementary material.

ACKNOWLEDGMENTS

We thank J. Cohen, C. Lupica, and G. Schoenbaum for comments on the manuscript; M. Myers Jr. for *Lepr^{Cre}* mice; M. Sharpe for behavioral assay assistance; T. Larson for imaging support; the NIDA IRP Histology Core for histology support; and the NIDA IRP Visual Media for brain drawings. Mouse clip art adapted from [Openclipart.org](https://openclipart.org) (Creative Commons CC0). Permission to publish the miniscope drawing was granted by Doric Lenses. The graphical abstract was created with BioRender.com. M.A.A. was supported by the NIDA IRP Scientific Director's Fellowship for Diversity in Research. This work was supported by the National Institute on Drug Abuse Intramural Research Program, US National Institutes of Health.

INCLUSION AND DIVERSITY

We worked to ensure sex balance in the selection of non-human subjects. One or more of the authors of this paper self-identifies as an underrepresented ethnic minority in science. One or more of the authors of this paper received support from a program designed to increase minority representation in science. The author list of this paper includes contributors from the location where the research was conducted who participated in the data collection, design, analysis, and/or interpretation of the work.

REFERENCES

- Allen BD, Singer AC, and Boyden ES (2015). Principles of designing interpretable optogenetic behavior experiments. *Learn. Mem* 22, 232–238. [PubMed: 25787711]
- Baladi MG, Koek W, Aumann M, Velasco F, and France CP (2012). Eating high fat chow enhances the locomotor-stimulating effects of cocaine in adolescent and adult female rats. *Psychopharmacology (Berl.)* 222, 447–457. [PubMed: 22418731]
- Barbano MF, Wang HL, Morales M, and Wise RA (2016). Feeding and Reward Are Differentially Induced by Activating GABAergic Lateral Hypothalamic Projections to VTA. *J. Neurosci* 36, 2975–2985. [PubMed: 26961951]
- Bonnavion P, Mickelsen LE, Fujita A, de Lecea L, and Jackson AC (2016). Hubs and spokes of the lateral hypothalamus: cell types, circuits and behaviour. *J. Physiol* 594, 6443–6462. [PubMed: 27302606]
- Brown JA, Woodworth HL, and Leininger GM (2015). To ingest or rest? Specialized roles of lateral hypothalamic area neurons in coordinating energy balance. *Front. Syst. Neurosci* 9, 9. [PubMed: 25741247]
- Brown JA, Wright A, Bugescu R, Christensen L, Olson DP, and Leininger GM (2019). Distinct Subsets of Lateral Hypothalamic Neurotensin Neurons are Activated by Leptin or Dehydration. *Sci. Rep* 9, 1873. [PubMed: 30755658]

- Chen TW, Wardill TJ, Sun Y, Pulver SR, Renninger SL, Baohan A, Schreiter ER, Kerr RA, Orger MB, Jayaraman V, et al. (2013). Ultrasensitive fluorescent proteins for imaging neuronal activity. *Nature* 499, 295–300. [PubMed: 23868258]
- Cunningham CL, Gremel CM, and Groblewski PA (2006). Drug-induced conditioned place preference and aversion in mice. *Nat. Protoc* 1, 1662–1670. [PubMed: 17487149]
- de Vrind VAJ, Rozeboom A, Wolterink-Donselaar IG, Luijendijk-Berg MCM, and Adan RAH (2019). Effects of GABA and Leptin Receptor-Expressing Neurons in the Lateral Hypothalamus on Feeding, Locomotion, and Thermogenesis. *Obesity (Silver Spring)* 27, 1123–1132. [PubMed: 31087767]
- Deacon RMJ (2006). Digging and marble burying in mice: simple methods for in vivo identification of biological impacts. *Nat. Protoc* 1, 122–124. [PubMed: 17406223]
- El-Brolsy MA, and Stainier DYR (2017). Genetic compensation: a phenomenon in search of mechanisms. *PLoS Genet.* 13, e1006780. [PubMed: 28704371]
- Giardino WJ, Eban-Rothschild A, Christoffel DJ, Li S-B, Malenka RC, and de Lecea L (2018). Parallel circuits from the bed nuclei of stria terminalis to the lateral hypothalamus drive opposing emotional states. *Nat. Neurosci* 21, 1084–1095. [PubMed: 30038273]
- Gomez JL, Bonaventura J, Lesniak W, Mathews WB, Sysa-Shah P, Rodriguez LA, Ellis RJ, Richie CT, Harvey BK, Dannals RF, et al. (2017). Chemogenetics revealed: DREADD occupancy and activation via converted clozapine. *Science* 357, 503–507. [PubMed: 28774929]
- Housden BE, Muhar M, Gemberling M, Gersbach CA, Stainier DY, Seydoux G, Mohr SE, Zuber J, and Perrimon N (2017). Loss-of-function genetic tools for animal models: cross-species and cross-platform differences. *Nat. Rev. Genet* 18, 24–40. [PubMed: 27795562]
- Itzhak Y, and Martin JL (2002). Cocaine-induced conditioned place preference in mice: induction, extinction and reinstatement by related psychostimulants. *Neuropsychopharmacology* 26, 130–134. [PubMed: 11751040]
- Jennings JH, Rizzi G, Stamatakis AM, Ung RL, and Stuber GD (2013). The inhibitory circuit architecture of the lateral hypothalamus orchestrates feeding. *Science* 341, 1517–1521. [PubMed: 24072922]
- Jennings JH, Ung RL, Resendez SL, Stamatakis AM, Taylor JG, Huang J, Veleta K, Katak PA, Aita M, Shilling-Scriver K, et al. (2015). Visualizing hypothalamic network dynamics for appetitive and consummatory behaviors. *Cell* 160, 516–527. [PubMed: 25635459]
- Krashes MJ, Koda S, Ye C, Rogan SC, Adams AC, Cusher DS, Maratos-Flier E, Roth BL, and Lowell BB (2011). Rapid, reversible activation of AgRP neurons drives feeding behavior in mice. *J. Clin. Invest* 121, 1424–1428. [PubMed: 21364278]
- Laque A, Yu S, Qualls-Creekmore E, Gettys S, Schwartzenburg C, Bui K, Rhodes C, Berthoud HR, Morrison CD, Richards BK, and Münzberg H (2015). Leptin modulates nutrient reward via inhibitory galanin action on orexin neurons. *Mol. Metab* 4, 706–717. [PubMed: 26500842]
- Leininger GM, Jo YH, Leshan RL, Louis GW, Yang H, Barrera JG, Wilson H, Opland DM, Faouzi MA, Gong Y, et al. (2009). Leptin acts via leptin receptor-expressing lateral hypothalamic neurons to modulate the mesolimbic dopamine system and suppress feeding. *Cell Metab.* 10, 89–98. [PubMed: 19656487]
- Leininger GM, Opland DM, Jo YH, Faouzi M, Christensen L, Cappellucci LA, Rhodes CJ, Gnegy ME, Becker JB, Pothos EN, et al. (2011). Leptin action via neurotensin neurons controls orexin, the mesolimbic dopamine system and energy balance. *Cell Metab.* 14, 313–323. [PubMed: 21907138]
- Leshan RL, Björnholm M, Münzberg H, and Myers MG Jr. (2006). Leptin receptor signaling and action in the central nervous system. *Obesity (Silver Spring)* 14 (Suppl 5), 208S–212S. [PubMed: 17021368]
- Li JX, Shah AP, Patel SK, Rice KC, and France CP (2013). Modification of the behavioral effects of morphine in rats by serotonin 5-HT_{1A} and 5-HT_{2A} receptor agonists: antinociception, drug discrimination, and locomotor activity. *Psychopharmacology (Berl.)* 225, 791–801. [PubMed: 22993050]

- Lu J, Li C, Singh-Alvarado J, Zhou ZC, Fröhlich F, Mooney R, and Wang F (2018). MINIPIPE: A Miniscope 1-Photon-Based Calcium Imaging Signal Extraction Pipeline. *Cell Rep* 23, 3673–3684. [PubMed: 29925007]
- MacLaren DA, Browne RW, Shaw JK, Krishnan Radhakrishnan S, Khare P, España RA, and Clark SD (2016). Clozapine N-Oxide Administration Produces Behavioral Effects in Long-Evans Rats: Implications for Designing DREADD Experiments. *eNeuro* 3, ENEURO.0219–16.2016.
- Mahn M, Prigge M, Ron S, Levy R, and Yizhar O (2016). Biophysical constraints of optogenetic inhibition at presynaptic terminals. *Nat. Neurosci* 19, 554–556. [PubMed: 26950004]
- McGuire BA, Baladi MG, and France CP (2011). Eating high-fat chow enhances sensitization to the effects of methamphetamine on locomotion in rats. *Eur. J. Pharmacol* 658, 156–159. [PubMed: 21371470]
- Mickelsen LE, Bolisetty M, Chimileski BR, Fujita A, Beltrami EJ, Costanzo JT, Naparstek JR, Robson P, and Jackson AC (2019). Single-cell transcriptomic analysis of the lateral hypothalamic area reveals molecularly distinct populations of inhibitory and excitatory neurons. *Nat. Neurosci* 22, 642–656. [PubMed: 30858605]
- Navarro M, Olney JJ, Burnham NW, Mazzone CM, Lowery-Gionta EG, Pleil KE, Kash TL, and Thiele TE (2016). Lateral Hypothalamus GABAergic Neurons Modulate Consummatory Behaviors Regardless of the Caloric Content or Biological Relevance of the Consumed Stimuli. *Neuropsychopharmacology* 41, 1505–1512. [PubMed: 26442599]
- Nieh EH, Matthews GA, Allsop SA, Presbrey KN, Leppla CA, Wichmann R, Neve R, Wildes CP, and Tye KM (2015). Decoding neural circuits that control compulsive sucrose seeking. *Cell* 160, 528–541. [PubMed: 25635460]
- Nieh EH, Vander Weele CM, Matthews GA, Presbrey KN, Wichmann R, Leppla CA, Izadmehr EM, and Tye KM (2016a). Inhibitory Input from the Lateral Hypothalamus to the Ventral Tegmental Area Disinhibits Dopamine Neurons and Promotes Behavioral Activation. *Neuron* 90, 1286–1298. [PubMed: 27238864]
- Oh SW, Harris JA, Ng L, Winslow B, Cain N, Mihalas S, Wang Q, Lau C, Kuan L, Henry AM, et al. (2014). A mesoscale connectome of the mouse brain. *Nature* 508, 207–214. [PubMed: 24695228]
- Qualls-Creekmore E, Yu S, Francois M, Hoang J, Huesing C, Bruce-Keller A, Burk D, Berthoud HR, Morrison CD, and Münzberg H (2017). Galanin-Expressing GABA Neurons in the Lateral Hypothalamus Modulate Food Reward and Noncompulsive Locomotion. *J. Neurosci* 37, 6053–6065. [PubMed: 28539422]
- Rescorla R, and Wagner A (1972). A theory of Pavlovian conditioning: Variations in the effectiveness of reinforcement and nonreinforcement. In *Classical Conditioning II: Current Research and Theory*, Black AH and Prokasy WF, eds. (Appleton-Century-Crofts).
- Rozeske RR, Jercog D, Karalis N, Chaudun F, Khoder S, Girard D, Winke N, and Herry C (2018). Prefrontal-Periaqueductal Gray-Projecting Neurons Mediate Context Fear Discrimination. *Neuron* 97, 898–910.e6. [PubMed: 29398355]
- Saunders A, Johnson CA, and Sabatini BL (2012). Novel recombinant adeno-associated viruses for Cre activated and inactivated transgene expression in neurons. *Front. Neural Circuits* 6, 47. [PubMed: 22866029]
- Schiffino FL, Siemian JN, Petrella M, Laing BT, Sarsfield S, Borja CB, Gajendiran A, Zuccoli ML, and Aponte Y (2019). Activation of a lateral hypothalamic-ventral tegmental circuit gates motivation. *PLoS ONE* 14, e0219522. [PubMed: 31291348]
- Schultz W, Dayan P, and Montague PR (1997). A neural substrate of prediction and reward. *Science* 275, 1593–1599. [PubMed: 9054347]
- Sharpe MJ, Marchant NJ, Whitaker LR, Richie CT, Zhang YJ, Campbell EJ, Koivula PP, Necarsulmer JC, Mejias-Aponte C, Morales M, et al. (2017). Lateral Hypothalamic GABAergic Neurons Encode Reward Predictions that Are Relayed to the Ventral Tegmental Area to Regulate Learning. *Curr. Biol* 27, 2089–2100.e5. [PubMed: 28690111]
- Sherwood A, Wosiski-Kuhn M, Nguyen T, Holland PC, Lakaye B, Adamantidis A, and Johnson AW (2012). The role of melanin-concentrating hormone in conditioned reward learning. *Eur. J. Neurosci* 36, 3126–3133. [PubMed: 22775118]

- Shin Yim Y, Park A, Berrios J, Lafourcade M, Pascual LM, Soares N, Yeon Kim J, Kim S, Kim H, Waisman A, et al. (2017). Reversing behavioural abnormalities in mice exposed to maternal inflammation. *Nature* 549, 482–487. [PubMed: 28902835]
- Steketee JD, and Kalivas PW (2011). Drug wanting: behavioral sensitization and relapse to drug-seeking behavior. *Pharmacol. Rev* 63, 348–365. [PubMed: 21490129]
- Stuber GD, and Wise RA (2016). Lateral hypothalamic circuits for feeding and reward. *Nat. Neurosci* 19, 198–205. [PubMed: 26814589]
- Thorn DA, Zhang C, Zhang Y, and Li JX (2014). The trace amine associated receptor 1 agonist RO5263397 attenuates the induction of cocaine behavioral sensitization in rats. *Neurosci. Lett* 566, 67–71. [PubMed: 24561093]
- Tooley J, Marconi L, Alipio JB, Matikainen-Ankney B, Georgiou P, Kravitz AV, and Creed MC (2018). Glutamatergic Ventral Pallidal Neurons Modulate Activity of the Habenula-Tegmental Circuitry and Constrain Reward Seeking. *Biol. Psychiatry* 83, 1012–1023. [PubMed: 29452828]
- Urstadt KR, and Berridge KC (2020). Optogenetic mapping of feeding and self-stimulation within the lateral hypothalamus of the rat. *PLoS ONE* 15, e0224301. [PubMed: 31986148]
- Yang CF, Chiang MC, Gray DC, Prabhakaran M, Alvarado M, Juntti SA, Unger EK, Wells JA, and Shah NM (2013). Sexually dimorphic neurons in the ventromedial hypothalamus govern mating in both sexes and aggression in males. *Cell* 153, 896–909. [PubMed: 23663785]
- Zhang X, and van den Pol AN (2017). Rapid binge-like eating and body weight gain driven by zona incerta GABA neuron activation. *Science* 356, 853–859. [PubMed: 28546212]

Highlights

- LH^{LEPR} neuronal ablation disrupts appetitive learning but not food intake
- Optogenetic manipulation of LH^{LEPR} neurons affects reward behavior but not feeding
- LH^{LEPR} but not LH^{VGAT} activity discriminates conditioned appetitive cues
- Modulation of LH^{LEPR} to VTA projections evokes divergent effects on learning

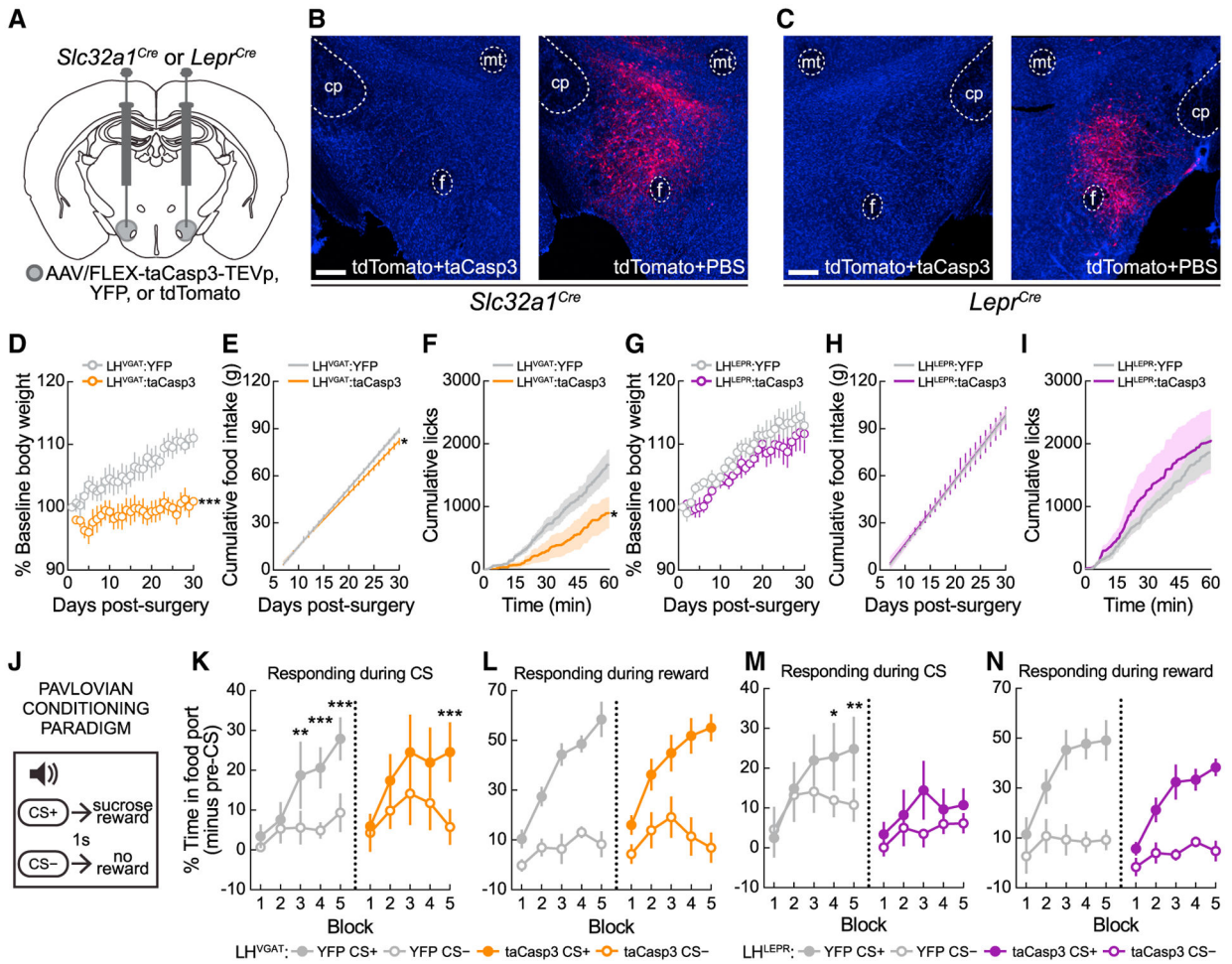


Figure 1. Cell-type specific ablation targeted to LH^{LEPR} neurons decreases appetitive but not consummatory behaviors

(A). Viral injection schematic.

(B and C) Representative images for taCasp3 ablation validation in the LH of *Slc32a1^{Cre}* or *Lepr^{Cre}* mice 30 days post-injection. Scale bars, 500 μ m.

(D) LH^{VGAT} ablation attenuated weight gain over 30 days. Two-way mixed-model ANOVA ablation \times day interaction ($p < 0.0001$), Bonferroni post-test: significant difference on day 30 ($p = 0.002$).

(E) LH^{VGAT} ablation attenuated daily ($p < 0.0001$) and cumulative food intake ($p = 0.037$) between days 7 and 30 post-surgery.

(F) LH^{VGAT} ablation decreased lick responses for a caloric liquid ($p = 0.039$).

(G) LH^{LEPR} ablation did not affect weight gain (2-way mixed-model ANOVA ablation \times day interaction, $p = 0.95$).

(H) LH^{LEPR} ablation did not attenuate daily ($p = 0.90$) or cumulative food intake ($p = 0.91$) between days 7 and 30 post-surgery.

(I) LH^{LEPR} ablation did not affect lick responses ($p = 0.75$).

(J) Pavlovian conditioning schematic.

(K) LH^{VGAT} ablation delayed but did not prevent appetitive learning. LH^{VGAT}:YFP mice: block \times CS interaction ($p = 0.0046$); significant main effects of block ($p = 0.0005$) and CS

($p = 0.0056$); Bonferroni post-test: discrimination during blocks 3–5 (** $p < 0.01$, *** $p < 0.001$). LH^{VGAT}:taCasp3 mice: main effect of CS detected ($p = 0.003$), Bonferroni post-test: significant discrimination by block 5 ($p = 0.0004$).

(L) LH^{VGAT} ablation did not affect pellet collection on CS⁺ trials ($p = 0.51$).

(M) LH^{LEPR} ablation prevented appetitive learning. LH^{LEPR}:YFP control mice block \times CS interaction ($p = 0.0219$); Bonferroni post-test: significant discrimination during blocks 4–5 (* $p < 0.05$, ** $p < 0.01$). LH^{LEPR}:taCasp3 mice failed to learn the task; no significant main effects of block ($p = 0.31$), CS ($p = 0.13$), or interaction ($p = 0.23$), and did not significantly discriminate stimuli by block 5 ($p = 0.50$).

(N) LH^{LEPR} ablation did not affect pellet collection on CS⁺ trials ($p = 0.87$).

Data represented as means \pm SEMs; $n = 6$ – 8 mice/group.

See also Table S1 for full statistics and Figure S1.

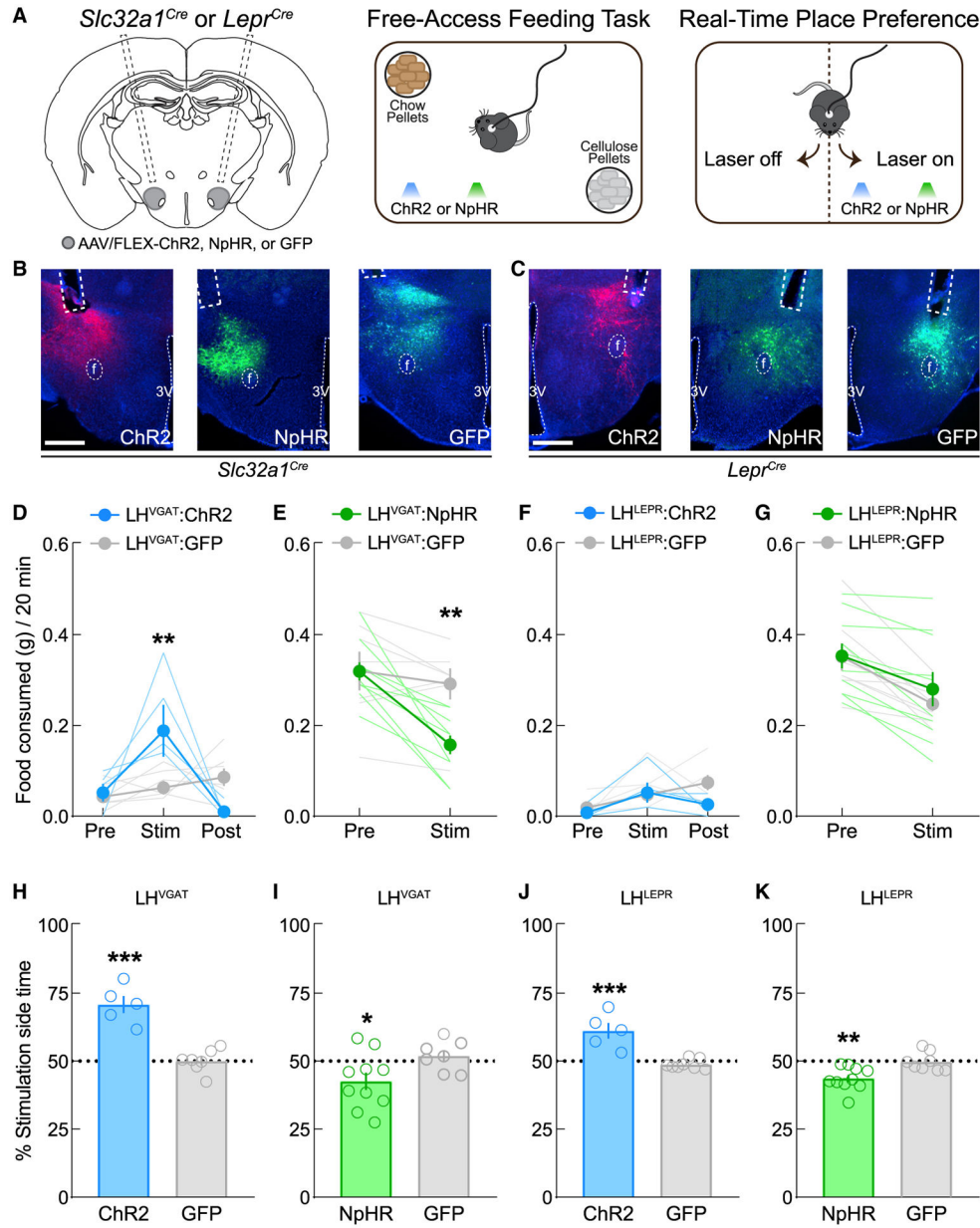


Figure 2. Optogenetic activation of LH^{LEPR} neurons does not evoke food intake but is rewarding
 (A) Schematics of viral injections, free-access feeding, and real-time place preference.
 (B and C) Representative images of ChR2, NpHR, and GFP in the LH and optical fiber placements above the LH in *Slc32a1^{Cre}* mice and *Lepr^{Cre}* mice. Scale bar, 500 μ m.
 (D) LH^{VGAT} neuron photoactivation triggers feeding. Two-way mixed-model ANOVA group \times epoch interaction ($p = 0.002$), Bonferroni post-test (** $p = 0.003$).
 (E) LH^{VGAT} neuron photoinhibition suppresses feeding. Two-way mixed-model ANOVA group \times epoch interaction ($p = 0.0027$), Bonferroni post-test (** $p = 0.005$).
 (F) LH^{LEPR} neuron photoactivation did not affect feeding. Two-way mixed-model ANOVA group \times epoch interaction ($p = 0.21$).

- (G) LH^{LEPR} neuron photoinhibition did not affect feeding. Two-way mixed-model ANOVA group \times epoch interaction ($p = 0.32$).
- (H) LH^{VGAT}:ChR2 mice displayed significant real-time place preference ($p < 0.0001$).
- (I) LH^{VGAT}:NpHR mice displayed significant real-time place aversion ($p = 0.045$).
- (J) LH^{LEPR}:ChR2 mice displayed significant real-time place preference over control mice ($p = 0.0003$).
- (K) LH^{LEPR}:NpHR mice displayed significant real-time place aversion ($p = 0.0049$).
- Data represented as means \pm SEMs; $n = 5$ – 10 mice/group.
See also Table S1 for full statistics and Figure S2.

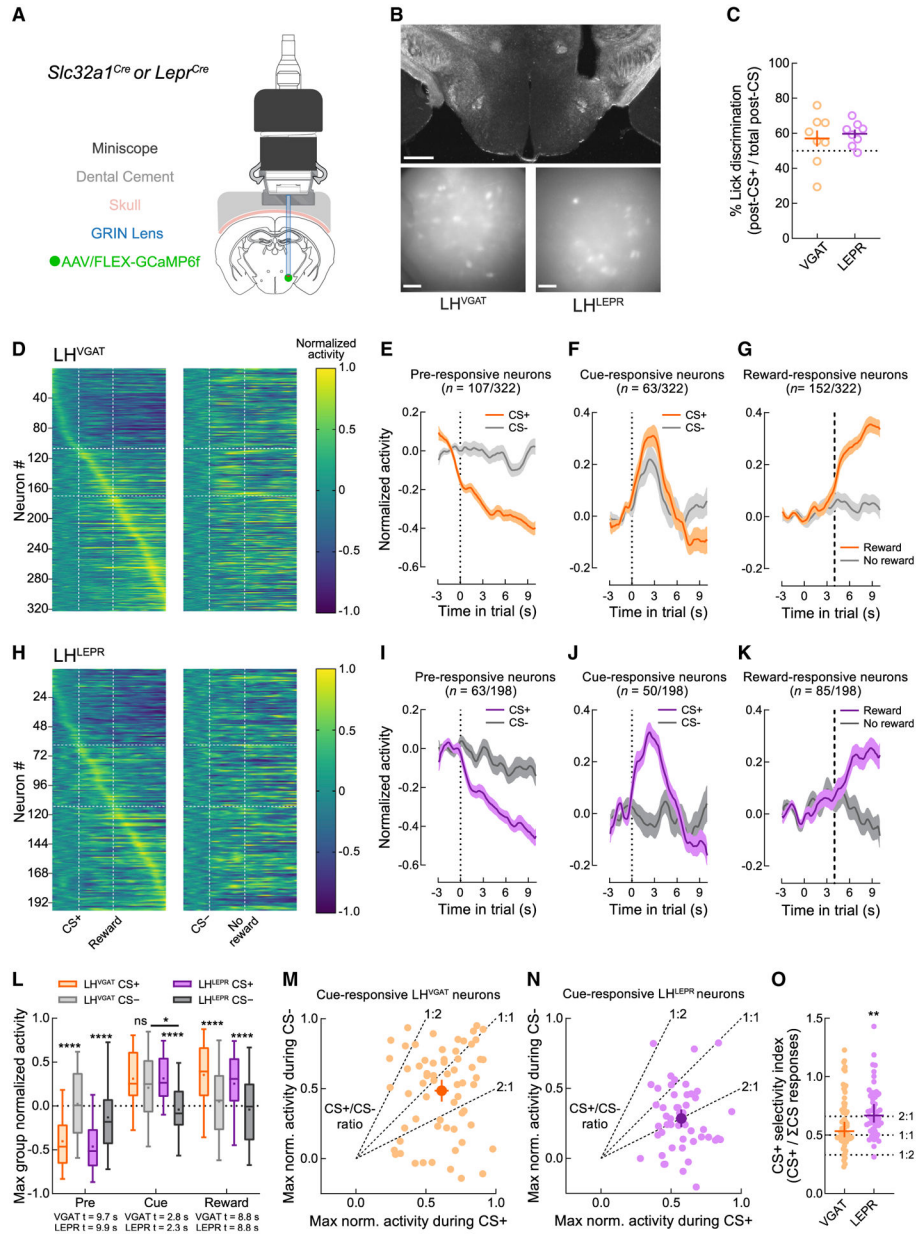


Figure 3. LH^{LEPR} neuronal activity discriminates reward predictive from non-predictive cues. (A) Schematic of deep brain calcium imaging. (B) Representative images of GRIN lens placement and field of view from *Slc32a1^{Cre}* and *Lepr^{Cre}* mice. Scale bars: top, 500 μ m; bottom, 100 μ m. (C) *Slc32a1^{Cre}* (n = 9) and *Lepr^{Cre}* (n = 8) mice used for functional imaging experiments on average performed most post-CS licks following CS⁺ trials. (D) Normalized Ca²⁺ traces of individual LH^{VGAT} neurons on CS⁺ or CS⁻ trials. Vertical dashed lines indicate the beginning of the CS and outcome epochs. Horizontal dashed lines indicate groupings of neurons according to the epoch of maximal activity. (E–G) Normalized traces of CS⁺ (orange) and CS⁻ (gray) trials of (E) pre-responsive, (F) cue-responsive, and (G) reward-responsive LH^{VGAT} neurons.

(H–K) Similar to (E)–(G), except for LH^{LEPR} neurons.

(L) LH^{LEPR} activity during the CS epoch discriminated trial types whereas LH^{VGAT} activity did not. * $p = 0.017$, **** $p < 0.0001$.

(M) Maximal activity of individual LH^{VGAT} neurons on CS⁺ and CS⁻ trials, without matching the sampled time bin. Dashed lines indicate sample CS⁺/CS⁻ ratios. The LH^{VGAT} centroid ratio was 1.26, indicating slight preference for CS⁺ trials.

(N) Similar to (M), but for LH^{LEPR} neurons; the centroid ratio was 2.00, indicating large preference for CS⁺ trials.

(O) CS⁺ selectivity index (CS⁺ response/ Σ CS responses) was higher for LH^{LEPR} than LH^{VGAT} neurons ($p = 0.0034$).

Data represented as means \pm SEMs.

See also Table S1 for full statistics.

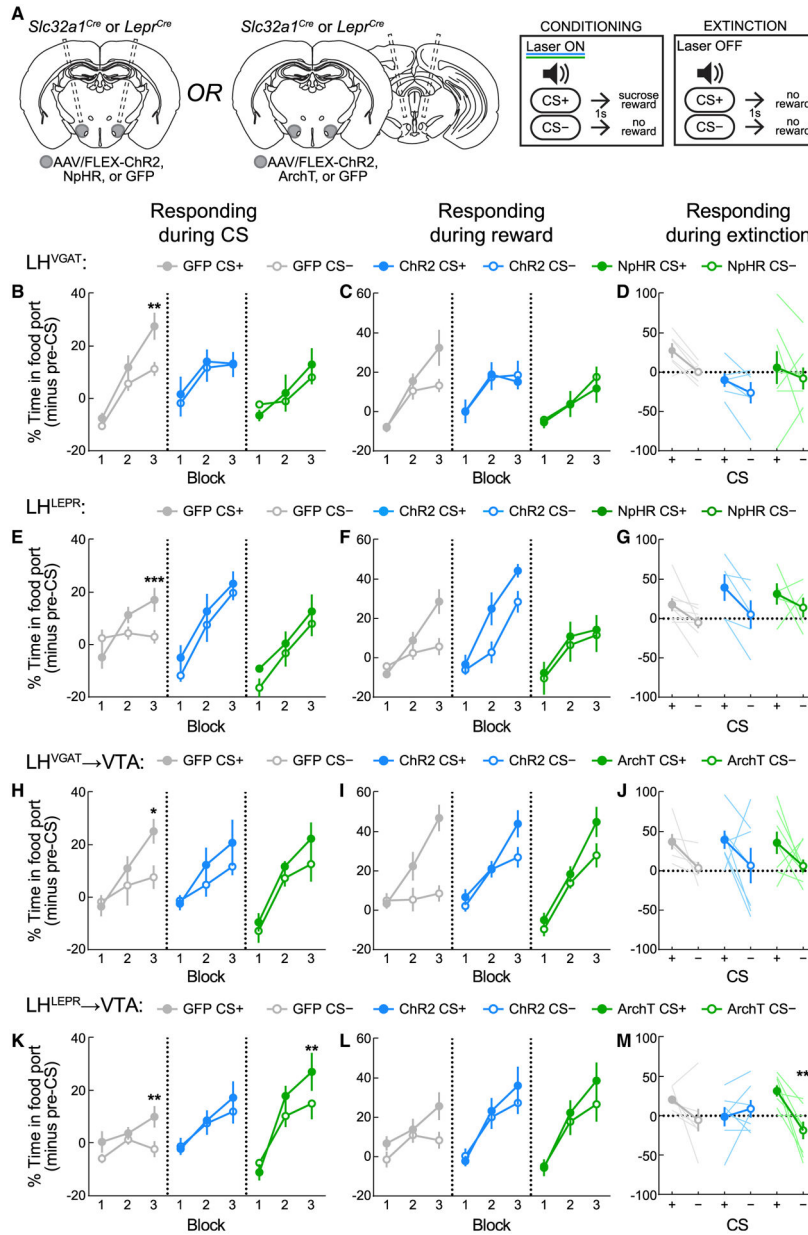


Figure 4. LH^{LEPR} neurons mediate appetitive learning via projections to VTA circuitry
 (A) Viral injection/implant schematics and Pavlovian training and extinction protocols.
 (B) Activation or inhibition of LH^{VGAT} neurons disrupts appropriate responding. LH^{VGAT}:GFP mice learned to discriminate CS⁺ from CS⁻. Activation of LH^{VGAT} disrupted conditioning, as did inhibition of LH^{VGAT} neurons. **p = 0.0021.
 (C) Intact sucrose pellet collection across LH^{VGAT} groups.
 (D) Discrimination between CS⁺ and CS⁻ was intact during the extinction test without optogenetic manipulation.
 (E) Activation or inhibition of LH^{LEPR} neurons disrupts appropriate responding. LH^{LEPR}:GFP mice learned to discriminate CS⁺ from CS⁻. Activation of LH^{LEPR} disrupted conditioning, as did inhibition of LH^{LEPR} neurons. ***p = 0.0007.

- (F) Intact sucrose pellet collection across LH^{LEPR} groups.
- (G) Discrimination between CS⁺ and CS⁻ was intact during the extinction test without optogenetic manipulation.
- (H) Activation or inhibition of the LH^{VGAT}→VTA pathway attenuates Pavlovian learning. LH^{VGAT}:GFP→VTA mice learned to discriminate CS⁺ from CS⁻. Activation of the pathway in LH^{VGAT}:ChR2→VTA mice or inhibition of the pathway in LH^{VGAT}:ArchT→VTA mice disrupted discrimination. *p = 0.017.
- (I) Retrieval of sucrose pellets was comparable across groups.
- (J) Discrimination between CS⁺ and CS⁻ was intact during the extinction test without optogenetic manipulation.
- (K) Inhibition of the LH^{LEPR}→VTA pathway enhances Pavlovian learning. LH^{LEPR}:GFP→VTA mice learned to discriminate the CS⁺ and CS⁻ (*p = 0.0063). While discrimination was not apparent in LH^{LEPR}:ChR2→VTA mice, LH^{LEPR}:ArchT→VTA mice displayed discrimination between cues in block 3 (*p = 0.0047).
- (L) Retrieval of sucrose pellets was comparable across groups.
- (M) Extinction test performance was significantly affected by LH^{LEPR}→VTA pathway manipulation during training (group × CS interaction, p = 0.017). Within-group discrimination of the CS⁺ and CS⁻ was abolished in LH^{LEPR}:ChR2→VTA mice (p > 0.99), but was increased in LH^{LEPR}:ArchT→VTA mice (p = 0.0032) as compared to controls (p = 0.27).
- Data represented as means ± SEMs; n = 5–8 mice/group.
See also Table S1 for full statistics and Figure S3.

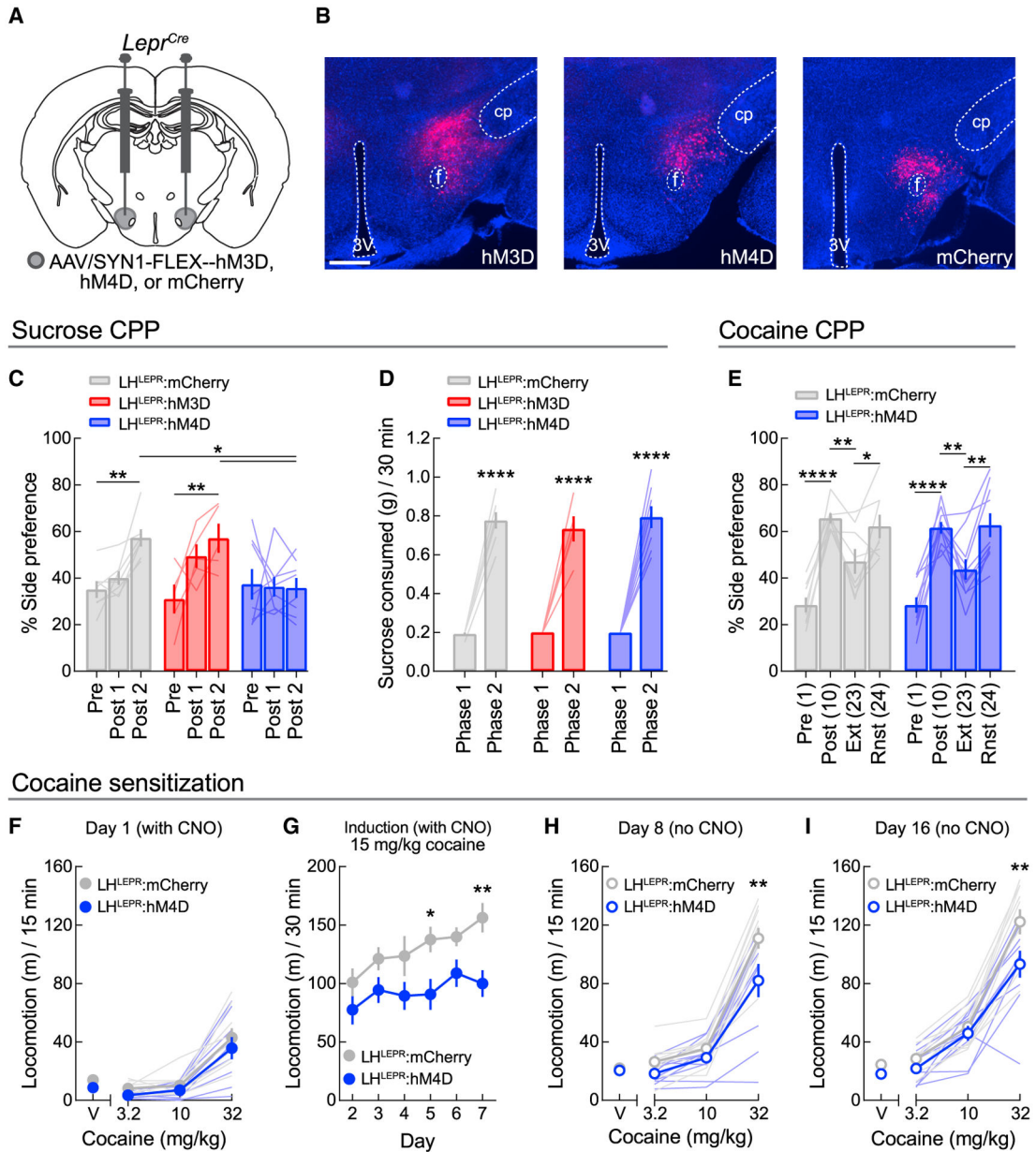


Figure 5. LH^{LEPR} neurons do not regulate cocaine-context learning

(A) Viral injection schematic.

(B) Representative images of hM3D, hM4D, and mCherry in the LH of *Lepr^{Cre}* mice. Scale bar, 500 μ m.

(C) Chemogenetic LH^{LEPR} manipulations did not affect phase 1 sucrose CPP (post 1), but inhibition blunted the development of CPP following phase 2 training ($p = 0.0136$). Bonferroni post-tests for LH^{LEPR}:mCherry (** $p = 0.0022$) and LH^{LEPR}:hM3D mice (** $p = 0.0023$) in post 2 as compared to pre. Sucrose-side preference was blunted in LH^{LEPR}:hM4D mice as compared to LH^{LEPR}:mCherry (** $p = 0.0049$) and LH^{LEPR}:hM3D mice (* $p = 0.0127$).

(D) Chemogenetic manipulations did not affect sucrose consumption in either conditioning phase. Each group consumed more sucrose during phase 2 training (**** $p < 0.0001$).

(E) Inhibition did not affect the induction of cocaine CPP or reinstatement following extinction. Pre, pre-test; Post, post-test; Ext, extinction test; Rnst, reinstatement test. * $p < 0.05$, ** $p < 0.01$, **** $p < 0.0001$.

(F) No acute effects of inhibition were observed on the locomotor-stimulating effects of cocaine.

(G) LH^{LEPR} inhibition during daily cocaine treatment blunted increases in locomotion. * $p = 0.043$, ** $p = 0.0078$.

(H and I) Prior LH^{LEPR} inhibition attenuated the locomotor-stimulating effects of cocaine following (H) 1 day and (I) 7 days cocaine abstinence; ** $p < 0.01$.

Data represented as means \pm SEMs; $n = 5-10$ mice/group.

See also Table S1 for full statistics and Figure S4.

KEY RESOURCES TABLE

REAGENT or RESOURCE	SOURCE	IDENTIFIER
Bacterial and virus strains		
rAAV2/1-EF1 α -FLEX-taCasp3-TEVp	Univ. of North Carolina (UNC) Vector Core	RRID:Addgene_45580
rAAV2/1-EF1 α -DIO-YFP	Karl Deisseroth, Stanford University	Addgene 27056-AAV9; RRID:Addgene_27056
rAAV2/1-CAG-FLEX-tdTomato	Oh et al., 2014	Addgene 51503-AAV1; RRID:Addgene_51503
rAAV2/9-CAG-FLEX-tdTomato	Univ. of Pennsylvania (Penn) Vector Core	RRID:Addgene_51503
rAAV2/1-CAG-FLEX-rev-ChR2-tdTomato	Penn Vector Core	RRID:Addgene_18917
rAAV2/5-EF1 α -DIO-eNpHR3.0-eYFP	UNC Vector Core	RRID:Addgene_26966
rAAV2/9-CAG-FLEX-ArchT-GFP	UNC Vector Core	RRID:Addgene_28307
rAAV2/9-CAG-FLEX-GFP	Oh et al., 2014	Addgene 51502-AAV9; RRID:Addgene_51502
rAAV2/9-hSyn-DIO-hM3D(Gq)-mCherry	Krashes et al., 2011	Addgene 44361-AAV9; RRID:Addgene_44361
rAAV2/9-hSyn-DIO-hM4D(Gi)-mCherry	Krashes et al., 2011	Addgene 44362-AAV9; RRID:Addgene_44362
rAAV2/9-hSyn-DIO-mCherry	Bryan Roth, UNC	Addgene 50459-AAV9; RRID:Addgene_50459
rAAV2/9-CAG-FLEX-GCaMP6f-WPRE-SV40	Chen et al., 2013	Addgene 100835-AAV9; RRID:Addgene_100835
Chemicals, peptides, and recombinant proteins		
cocaine hydrochloride	NIDA Drug Supply Program	N/A; PUBCHEM:656832
clozapine- <i>N</i> -oxide (CNO)	Toctris Bioscience	Cat#4936; PUBCHEM:135445691
Experimental models: organisms/strains		
Mouse: <i>Lep^{tm3(cre)Mgmj} (Lep^{Cre})</i>	Leshan et al., 2006	RRID:MGI:381324
Mouse: <i>Slc32a1^{tm2(cre)Low1} (Vgat^{Cre})</i>	The Jackson Laboratory	RRID:IMSR_JAX:028862
Mouse: <i>Gt(ROSA)26Sor^{tm3(CAG-EYFP)Hze} (Rosa26^{YFP})</i>	The Jackson Laboratory	RRID:IMSR_JAX:007903
Software and algorithms		
GraphicState v4	Coulbourn Instruments	Cat#GS4.0
ANY-maze behavioral tracking software v5	Stoelting Co.	https://www.any-maze.com
MATLAB	MathWorks	R2020a; RRID:SCR_001622
MIN1PIPE	Lu et al., 2018	https://github.com/JinghaoLu/MIN1PIPE
Prism 8	GraphPad	RRID:SCR_002798
Neuroscience Studio v5.1	Doric Lenses, Inc.	RRID:SCR_018569
Other		
PicoLab Rodent Diet 20 (5053) Pellet – 20 mg Pellet	LabDiet	Cat#1815928–372
Calorie-Free Reward Pellet 5TUW – 20 mg Pellet – No Flavor	LabDiet	Cat#1811557
Sucrose Reward Pellet 5TUT – 20 mg Pellet	LabDiet	Cat#1811555
Ensure Original Vanilla Nutrition Shake	Abbott	N/A
Basic Fluorescence Snap-In Microscopy System - Deep Brain	Doric Lenses, Inc.	N/A

REAGENT or RESOURCE	SOURCE	IDENTIFIER
Snap-In Imaging Cannula Model L-V	Doric Lenses, Inc.	N/A

Author Manuscript

Author Manuscript

Author Manuscript

Author Manuscript